Journal of Harbin Engineering University
ISSN: 1006-7043

Vol 44 No. 10
October 2023

Breast Cancer Diagnosis in Full Field PET: A Successful Method Using Two Full and Cropped Detection Paths and An Optimal Faster R -CNN

Mrs. S. Tharani[1*], Dr. R. Khanchana[2],

[1*]Reasearch Scholar & Assistant Professor, Department of Computer Science, Sri Ramakrishna College of Arts & Science for Women, Coimbatore, E-mail Id: vtharani1811@gmail.com
[2]Associate Professor, Department of Computer Science, Sri Ramakrishna College of Arts & Science for Women, Coimbatore, E-mail Id: khanchanacs@srcw.ac.in

***Corresponding Author:** Mrs. S.Tharani
*Reasearch Scholar & Assistant Professor, Department of Computer Science, Sri Ramakrishna College of Arts & Science for Women, Coimbatore, E-mail Id: vtharani1811@gmail.com

Abstract:

Medically, it is crucial for discovering breast cancer in its earliest stages order to lower mortality. Two different kinds of PET tumorsmass and calcification can be classified as benign or malignant using a new computer-aided detection (CAD) and classification technique. This study examines possibilities for diagnosing and categorising breast lesions by integrating multi-modality radiomics data from positron emission tomography (PET) and magnetic resonance (MR) images to characterise breast cancer phenotype and prognosis. an OFRCNN system that locates lesions in complete and cropped PET images and then classifies themselves to determine their pathology type. The system combines the Reinforced Marine Predators Algorithm (RMPA) with an Optimal Faster Region with Convolutional Neural Networks (OFRCNN) to determine the great values for the hyperparameters of the FRCNN structure. The full-field digital PET scans from the QIN-Breast dataset are used to apply the three steps of the suggested technique. The PET images are first cleaned up in advance to get rid of any extraneous artefacts, and then they are cut into thin, overlapping slices. Second, after establishing the OFRCNN model, masses are located using two different methods: full PET detecting and cropped slice detection. The outcomes demonstrated that the OFRCNN performed better than its competitors.

Keywords: Breast Cancer, Computer-Aided Detection, Reinforced, Marine Predators Algorithm, Classification Diagnosis.

Introduction

India has a low but rising mortality rate for breast cancer. The largely prevalent malignancy in urban Indian women and the next most frequent in rural women is breast cancer [1]. Because of the lack of cognizance and absence of a breast cancer screening programme, a significant amount of breast cancers is found at a rather complicated level. The current level of care for treating breast cancer varies significantly with respect to where a patient obtains treatment. According to epidemiological research, the number of people with BC worldwide is forecasted to reach about 2 million by the year 2030 [2]. From 1965 and 1985 in India, cases rose considerably, by about 50% [3]. There were in excess of 118000 incident instances in 2016; 526000 of these cases were common, and 98.1% of them involved females. Each state in this country has witnessed a rise in the average age of BC in women during the preceding 26 years, which makes up 39.1%[4]. As stated by Globocan data for 2020, BC caused 10.6% of all deaths and 13.5% of cases of cancer in India, with a lifetime risk of 2.81 [5], as shown in Fig.1.

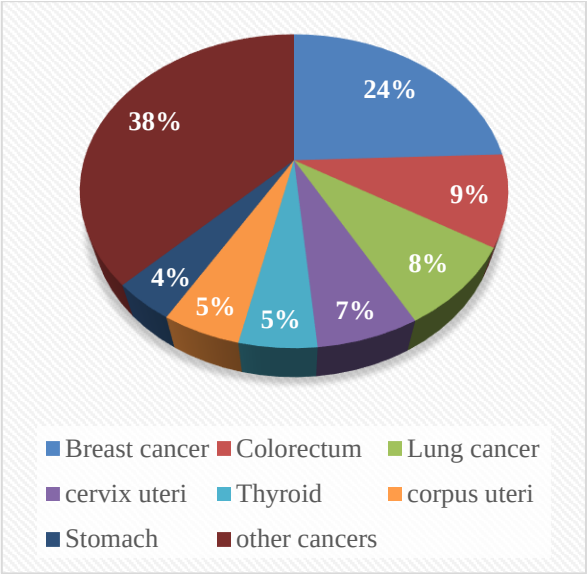

Fig.1. Pie chart of Estimated number of new cancer cases in 2020, worldwide by World Health Organization. [6]

Although BC cannot be prevented, the result can be greatly enhanced by early identification. This can also considerably cut the expense of the medical care. To find any initial anomalies before the tumour becomes progressed, mammography and

self-breast exams are essential [7]. Although mammography is still the primary imaging test used for identifying and screening cancer, other secondary imaging modalities are additionally in use, such as MRI, ultrasound, PET/CT, which can show strange metabolic activity.The benefits of PET/CT as an additional imaging modality for assessment of individuals with breast cancer is reviewed in this study [8]. As a result, the suggested method chooses to use mammographic datasets to find any current tumours. Although numerous improvements have been made to the current CADs to improve the precision of detection, there are still several obstacles in the way. Either the developing CADs or the mammography features reflect these difficulties. Due to their lengthy detection times, the primary issues with currently available CADs are reflected in their inability to be applied to real-world systems employed by hospitals or laboratories [9].

Machine learning is the method employed most frequently in studies [10]. Decision trees, KNN, SVM, naive bays, and other machine learning algorithms performed well. Still, the created method is utilised to categorise breast cancer. Deep learning is used to overcome the drawbacks of machine learning. Recurrent neural networks, Convolution neural networks, deep belief networks, and other deep learning techniques are frequently used. Deep learning algorithms achieve superior to machine learning algorithms. The best characteristics of the images are extracted. CNN is utilised to categorise the photos in recent research [11]. Essentially, the study uses PET pictures, and CNN is the most widely used method of classifying the images.

In this study, a real-time CAD system based on the newly developed full PET cropping and merging method is presented. It can locate masses quickly and accurately. Two pathways make up the suggested framework. The first route involves sending system the complete PET after scaling it to localise masses. The second approach involves cutting the whole PET into thin slices without resizing the original PET, detecting any current masses in the sliced portions, and then merging the sliced portions to obtain any diagnosed lesions loss using the full PET in the first phase. OFRCNN is used to identify tumours in the breast using two methods: complete cropped detection paths. The localised lesions it obtains are then classified by replacing the FRCNN's categories with other feature extractors, and the hyperparameter optimisation is performed using RMPA. The deficiency in the number of PET datasets that are freely accessible is remedied by implementing the suggested design based on the cropping approach. Additionally, the suggested PET cropping idea is successful in maintaining the high-resolution quality of the PETs by cutting each whole PET into several small slices to match the OFRCNN algorithm in an experiment to prevent losing any data by downsizing the complete PETs. The crossed slices also lead to the discovery of certain missing lesions that would not have been picked up by a comprehensive PET scan. Along with the radiologists' choices to verify the localised lesions and the first layer full PET diagnosis decision, the new cropping suggestion also serves as a third reader. The presented work's feature extraction classifiers and OFRCNN are both employed to categorise the discovered tumours. The effectiveness of each is compared as a means to determine which classification model is most appropriate for using to identify the pathology type of localised lesions.

The rest of the article is classified as follows: The relevant research to the developed techniques for breast cancer discovery and categorization is presented in Section II. The specifics of the two-detection procedure for aberrant lesions and the categorization phase for localised masses are then introduced in section III. The suggested technique's efficiency is discussed in section IV along with comparisons to other recent works in the field of breast cancer localisation, and section V concludes the work with suggestion for later research.

Related Work

The computer-aided diagnosis (CAD) methods for detecting breast cancer that have recently been created and have undergone peer review are included in this category. Using more than 200000 exams (more than 1000000 images),

Wu et al. [12] demonstrated a deep convolutional neural network (ResNet) for classifying breast cancer screening exams. When evaluated on the population undergoing screening, the network successfully predicts the existence of breast cancer with an AUC of 0.895. On high-dimensional data does notperform well.

Hamed et al., [13] suggested CAD system with a YOLOV4 foundation that can localise lesions in both complete and cropped mammograms and categorise according to the pathology type. The full-field digital mammograms from the INbreast dataset are subjected to three steps of the suggested technique. In a study intended to prevent data loss by downsizing the enhanced mammograms, the results demonstrate the influence of using YOLO-V4 as a sensor with the two paths of recognition of a full mammography and the cropped parts. The location of the masses is successfully detected by the suggested approach with a 98% overall accuracy. its accuracy of about 95% in differentiating among benign and malignant tumours. But this CAD-stained diagnosis is time-

consuming and requires a lot of work from knowledgeable professionals.

Zheng et al., [14] suggesteda Deep Learning assisted Efficient Adaboost Algorithm (DLA-EABA) has been theoretically developed using cutting-edge computational methods. Deep convolutional neural networks (CNNs) are utilized to build tumour categorization algorithms that utilise transfers along with to conventional computer vision techniques. The results expose that, a precision level of 97.2%, Specificity 96.5%and Sensitivity 98.3%, has been achieved. However, the CAD systems' accuracy is still insufficient.

Wang et al., [15] suggested a CNN deep features and unsupervised extreme learning machine (ELM) clustering. create a feature set by combining texture, density, morphological, and deep features. Then, an ELM classifier is created to characterize breast masses. The outcomes exhibit the precision and productivity of the suggested mass identification and categorization technique, but in the images dataset it doesn't give better results.

Nagalakshmi [16] suggested a transfer learning model was combined with various pre-trained CNN structures to create an Ensemble-Net model, which was utilized to separate the PM border from the rest of the breast in mammograms. In addition, it uses global mean pooling and softmax categorization to decide among malignant and benign malignant instances. Moreover, the results show the Ensemble-Net outperforms other traditional classifiers in accuracy, achieving 96.72%. However, it is still challenging without separating the rest of the breast area from the pectoral muscle (PM) boundary.

Bhausaheb& Kashyap [17] implemented a deep CNN based on Deer-Canids to identify malignant,benign, and normal regions in order to diagnose breast cancer. The effectiveness of the suggested Deer Canid optimization-based deep CNN was demonstrated by assessing its precision,accuracy, f1 measure and recall. It achieved the more optimal values of 92.967%, 94.342%, 93.454%, and 92.896%. But initialidentification of the conditionsare the only workable way to lessen the illness's effect.

Oyetade et al., [18] developed a Deep convolutional neural network (DCNN) with fuzzy support vector machines are used in both two-class and three-class models for the identification and categorization of breast cancer. For binary forecasts, the first layer of the serial 2-layer DCNN with fuzzy SVM produced accuracy of 99.61% and 100%, accordingly. The second layer provided 86.60% and 91.65%, accordingly. These systems are primarily designed for either binary classification or three-class classification and are subject to mistakes or erroneous.

Chattopadhyay et al., [19] suggested a complete deep learning model for diagnosis from histopathology images called Multi-scale Dual Residual Recurrent Network (MTRRE-Net). The suggested approach has been tested using dataset called BreaKHis, and it outperformed current models with excellent accuracy on every image considered at different magnification levels. But a smaller dataset can benefit from using such a network.

Proposed Methodology

The examination approach and recommended structure phases for classifying and detecting lesions in PET scans are addressed. The planned structure is separated into three phases, as depicted in Fig. 1. The pre-processing phase gets the PET images to setup without any unnecessary artefacts. The second phase, known as recognition, oversees setting up OFRCNN to locate masses in the aberrant images using two different detection methods. The third phase is the classification phase, which involves using different feature extractors in place of the OFRCNN categories to determine whether discovered lesions are benign or malignant. The entire design of the OFRCNN-based recognition structure is revealed in Fig. 1.The special parameters of OFRCNN design are optimised using the RMPA.

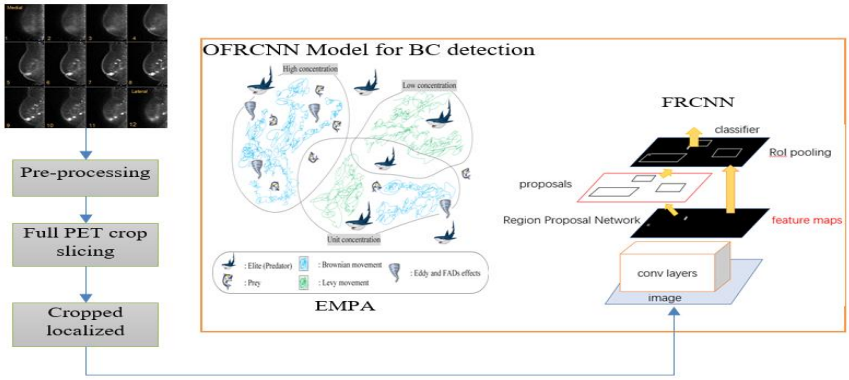

Fig.2. OFRCNN Model for BC detection

Input image database

This group includes longitudinal PET/CT and statistical MR images that were gathered to research therapy evaluation in neoadjuvant breast cancer. Three time points were used to obtain the images: before the first cycle of therapy (t1), afterward the first cycle of medications (t2), andafterward the second cycle of medication or when all treatments had been completed (before surgery) (t3). A support system that was created in-house allowed the individual to be in a prone state during the acquisition of the PET/CT images, which made it easier to register them with the MRI data. This collection's usefulness is in providing medical imaging info for the creation and estimation of measurable imaging techniques to assist with evaluation prior to the development of cure for breast cancer.The Imaging Data are FDG-PET/CT imaging, DCE, DWI, and T1 Mapping MRI images.Number of subjects / images: 68 subjects and **Link to dataset / homepage:** https://wiki.cancerimagingarchive.net/display/Public/QIN-Breast. The database contains 214 studies, 530 number of series, 100835 images and has 11.286GB image size.

Image Pre-processing

The primary task for healthcare imaging is pre-processing since it identifies aberrant parts that cannot be seen by visualising the image but can be seen by CAD systems. Here, undesirable artefacts were removed during pre-processing to improve the image quality. Pre-processing of PET investigated that the effectiveness of the CAD system is influenced by the choice of critical factors for quality improvement [20]. The pre-processing procedures are displayed in Figure 4.

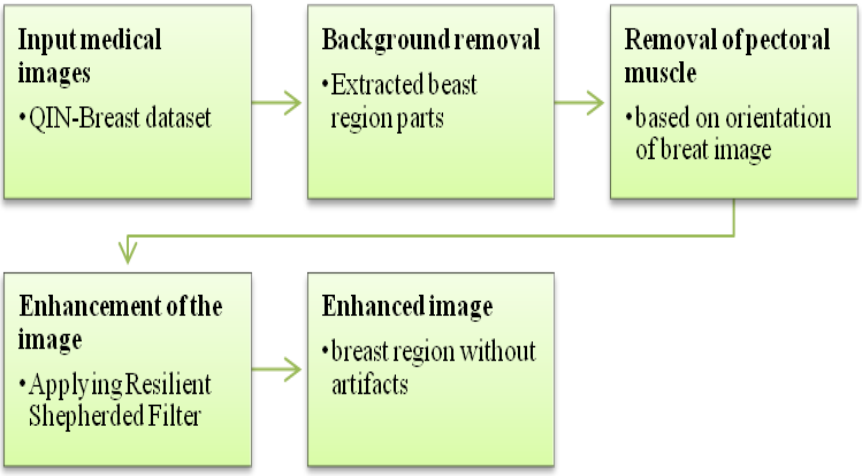

Fig.3. SmartArt of Steps carried out in pre-processing of PET image

Histogram based background removal: The standard approach for detecting the threshold value from a histogram with the background of a mammogram eliminated is to use the histogram. The breast feature was defined by the greatest component after picture binarization and ordering with related elements using the established threshold value [21].

Pectoral Muscle Removal: The excision of the pectoral muscle during mammography pre-processing is a further challenge [22]. The pectoral muscle was removed using the altered region-growing technique by determining whether the illustration was left- or right-oriented at its inception. Following the determination of the origin, the pectoral muscle is divided using the first pixel from the top corner as a seed point. This procedure is repeated until the entire muscle component is noted.

Image enhancement Using Robust GuidedFilter (RGF): Introduce the RGF linear filter in this chapter. RGF can be utilised for normalising and categorising the raw PET picture since it has excellent edge-preserving and detail-enhancing characteristics, much like the Gabor Filter method. The RGF filter utilises various filter kernel weights KW than the adaptive directed filter (AGF) proposed [24]. This part also discusses a flexible parameter setup technique that improves the RGF's suitability to analyse PET pictures. RGF performs better than most suggested filters in regards to edge retention and computational performance. By incorporating a resilient coefficient into the RGF may be utilised to convey the denoising efficiency and the capacity to maintain the genuine PET data

$$KW_{RSF_{ij}}(\mathfrak{G}) = \frac{1}{|\omega|^2}\sum_{i,j\in\omega_k}\left(1+\frac{\left(((\mathfrak{G}_i+\varphi_i)-\mathsf{C}_k)(\mathfrak{G}_j-\vartheta_k)\right)}{\beta_k^2+\epsilon}\right) \quad (1)$$

Where $\mathfrak{G}_i$guidance image and the coefficients $\mathsf{C}_k$and $\vartheta_k$are constant in window ω_k, whose width of the range filter can be calculated by minimising the variation in the output and input images. β_r is also locally adaptive.The window's central pixel that is currently being processed asω_k,parameters C_k and

$\vartheta_k$are essential for the RGF, which chooses when to smooth out or retain a specific region of an image.The coefficients can be calculated using a linear regression model, and φ_i is the additional offset, which is controlled by the equation below. $\epsilon = 0.1^2$ is a regularisation parameter to avoid C_k from being too large.

$$\varphi_i = \begin{cases} \max(\omega_k) - \mathfrak{G}_i & \mathfrak{y}_i > \max(\omega_k) \\ min(\omega_k) - \mathfrak{G}_i & \mathfrak{y}_i > \min(\omega_k) \\ \mathfrak{z}_i & otherwise \end{cases} \quad (2)$$

where the GF serves as the immediate source of $\mathfrak{y}_i = \mathfrak{G}_i + \mathfrak{z}_i$ and $\mathfrak{z}_i$. As a result, the output is guided by a crisper image, and the pixels along an edge are practically improved. The slope is increased by the RGF's edge preservation characteristics; however this causes significant overshoot and undershoot. Despite producing overshoot and undershoot around the edges, the RGF bestows detail and edges.

Masses Detection Based on Full PETs Detection and Cropped PETs Detection Phase

According to most current study for the identification of breast cancer, entire PET scans are shrunk down from their original vast dimensions to match one of the voracious deep learning algorithms [25]. The major symptoms of the resizing problem are a decline in image resolution and the absence of some important details, particularly when the resizing was done by a big factor. OFRCNN is one method utilised here to discover to localise tumours in PET images out of two that are utilised for identifying tumours: the complete PET identification and the cropped slices detection.

Full PETs Detection Phase (FPDP): In addition to the negative samples of the normal PETs, the PETs are divided into 3 classes: benign, malignant, and normal. But in the following technique, the PETs are classified into two classesnormal and abnormalin addition to the regular ones (regardless of the pathology kind). The dataset is split into 20% for testing and 80% for training in both strategies. The Algorithm of Full PETs Detection Phase is given in Table 1.

Table 1. Algorithm of Full PETs Detection Phase

Input: All PET images
Output: pathology type
Divided into 20% for testing and 80% for training
Obtain slices result from Cropped PETs Detection Phase
Train OFRCNN using the cancer slices vs normal slices
There are three types of PETs: malignant, normal and benign.

Cropped PETs Detection Phase (CPDP): This path's goal is to analyse a particular example to find any missing masses that path 1 was unable to identify. There are three primary steps in the second identification path. Each massivePET is first cropped into thin portions. In order to verify for any lesions PET scans and to be utilised in the structure detection assessment, these short slices are secondly stored for input to OFRCNN for training. These slices are subjected to the identification process in order to determine whether lesions (which would be abnormal) are present in new tiny PET scans. The thereafter of each PET slice to obtain the existing masses bounding boxes on the combined entire PET is the final significant step. In abnormal factors, the tumour is discovered without recognising what form of cancer it is, or in regular PET scans, nothing is seen. The Cropped PETs Detection algorithm is exhaustive in Table 2.

Table 2. Algorithm of Cropped PETs Detection Phase

Input: Full PET image
Output: The result of slices
Set cropping parameters width and height as (224, 448, 832,1024)
Set overlapping ratio between slices (50%)
Set neglection ration and check condition that if it contains small part of mass or black area>=75%
Then neglect that part
Else crop the PET into small slices
If a mass exists in this slice, then
Consider it normal
Else
Recalculate the mass coordinates to fit new slice coordinates
Produce slice result of PET

Detection Intersection Rules of FPDP and CPDP for the lesion's localization

the newly presented detection pathways are combined to examine for any lesions in the image analysed PET. The CPDP is suggested which improves its identification efficiency since it is successful in obtaining most of the lesions discovered by the FPDP along with to those not gotten by the FPDP. By employing the suggested method, a third supporter to the last judgement that was reflected in the CPDP established via the results that it could to read as a third reader to a particular mammographic case. Typically, CADs up until now read as a second reader in addition to radiologist'

choices. Since it considers the PET as a single unit with all the traits and attributes incorporated, the FPDP is typically the primary reference for the choice. Given the structures and colour intensities are comparable to those of the breast, dense PETs or PETs including tumours that are not visible call for the use of the CPDP. To get suspicious areas in PET scans, the findings from both detection routes are merged as indicated in Table 3:

Table 3. Algorithm of Cropped PETs Detection Phase

Input:FPDP and CPDP resultant images
Output: The result of localization of lesion
Get the output of FPDP using best weights obtained from CPDP
GET the preprocessed PET and cropped into slices using CPDP with size 1024 × 1024 and get lesions localization
The generated slices are then post-processed in order to be combined and obtain full PET.
Obtain any intersecting localised lesions among the results of the FPDP and the CPDP to be treated as a proven malignant case, i.e. ‘‘Confirmed localized masses’’ = ‘‘FPDP Detections Results’’ ∩ ‘‘CPDP Detections Results’’.
If no results are obtained from CPDPbut there are ‘‘FPDP Detections Results’’
Then take FPDP as a final result
else
do step 4
If no results are obtained from FPDP but there are ‘‘CPDP Results’’, then the confidence score (CS) of the gained masses will be patterned to take only those that their CF ≥ 0.5.
Else do step 4
End Process

Masses Classification Phase Using OFRCNN

Since the yield in cases of irregular PETs is the tumor's bounding box rather than distinction among malignant and benign tumours, both the second method of the FPDP and the CPDP are both used. The collected tumours must therefore be classed as malignant or benign in order to be capable to provide a comprehensive identification and categorization technique and for assessing the suggested study's efficiency with others. the mass area is divided into different images using a vector of coordinates that represents the bounding box of the actual masses. other feature extractors take up the duty of the OFRCNN in classifying lesions after they have been localised.

FRCNN: FRCNN is a technique utilising deep learning to recognise objects that was created from the R-CNN algorithm to address the flaws in R-CNN [26]. It is frequently used for recognising objects. A neural network called the RPN takes the place of a targeted search to suggest regions. Since the procedure takes a long time to analyse images—roughly two seconds each image—selective search is no longer necessary. Because RPN processing is not repeated, as it is in R-CNN, the entire model can be developed from beginning to end. RPN serves to construct several bounding boxes, with each box having two probability scores indicating if there are lesions at that place or not. Initially it incorporates all models into a single network that comprises of extraction of features, categorization, and identification, unlike R-CNN. The next step CNN only needs to run once per image instead of once per region. A layer known as the Region of Interest (RoI) pooling layer is where all areas share these CNN features (i.e., a conv feature map). Essentially, a convolution feature map's RoI is a rectangular window. The characteristics of each region are the result of RoI pooling (i.e. employing max pooling). A review of the Region Proposal Network Layer (RPN), the important layer in the FRCNN.

RPN Layer: Typically, FRCNN generates region suggestions and detects objects using similar feature maps. region proposals are created and lesions are detected using a shared CNN. When analysing the yield of the last convolutional layer of the VGGNet, which includes n cells with 512 feature mappings each, the lesions are where these ideas are created. The kernel over a convolutional feature map produces a 1D representation if a tiny network window is used, or a 3×3 kernel around a single cell. A 512-dimensional model for this position will be offered if this method is repeated for all 512 feature maps.For each of the $\mathfrak{w} \times \mathfrak{h}$ positions, this procedure yields a 512-dimensional representation. Given that the first layer is a box-regression layer (brl) and the second is a box-classification layer (bcl), this vector will feed two fully linked layers [27]. The sliding window's pivotal point is the anchor. The two crucial factors for each image are the aspect ratio, the ratio of the image's width to its height and the scale factor. The approach selects 3 scales and 3 aspect ratios. Nine proposals in total are produced for each location as a result. The anchor is determined by considering each regional anchor's K=3 scale, 3×3 aspect ratio, and 9.The number of anchors for the complete image is $\mathbb{W} \times \mathbb{H} \times \mathbb{K}$, whereas the size of the feature map is the feature map of size $\mathbb{W} \times \mathbb{H}$. The Intersection Over Union (IOU) for each region, which will be discussed in the next part, determines which anchor to use. With

respect to a ground truth box, tocontemplate the anchors with the greatest IOU overlap, where the IOU Overlap must above a particular predetermined threshold. employed categorical cross entropy as a loss function. It can be calculated using the formula below:

$$CCE(\mathfrak{pv}, \mathfrak{tv}) = -\sum_{\mathfrak{c}=1}^{\mathfrak{C}} \mathfrak{tv}_{\mathbb{O},\mathfrak{c}} \cdot \log\left(\mathfrak{pv}_{\mathbb{O},\mathfrak{c}}\right) + \tau \sum_{\mathfrak{c}=1}^{\mathfrak{C}} \mathbb{p}_i \times log\left(\mathfrak{tv}_{\mathbb{O},\mathfrak{c}}\right) \quad (3)$$

Where $\mathfrak{C}$ is the number of classes,$\mathfrak{tv}$ is the target value, $\mathfrak{pv}$ is the predicted value,$\mathbb{O}$ represents observation, i is the index of an anchor, $\mathbb{p}_i$is the predicted probability of anchor andτ is abalancing parameter.

IOU: a metric used to determine which images detect lesions. By splitting the overlapping area across the region of union among both, it effectively assesses the overlayamongthe ground truth and the anticipated bounding box. By defining a threshold, a prediction will only be deemed accurate if IOU>threshold (0.7) for each bounding boxand it is calculated using formulas as follows $IOU = area\ of\ overlap/area\ of\ union$. The definition of IoU as a function that accepts two bounding boxes is included in the implementation. In order to discover the best match for each ground truth bounding box, non-maximum suppression (NMS), a filter, iterates through predicted bounding boxes. The remaining predicated bounding boxes in this region are eliminated, and only the finest match is saved. [28] breaks down the FRCNN process into three key parts, note that the inputs might be any size image. The result is what is known as a "objectless score," which is a set of rectangle proposals for each object with a likelihood of lesions for each suggestion.

- The primary layer is the CNN layer, which take the key characteristics and extract them for the subsequent layers (RPN and R-CNN).
- The Region Proposal Network (RPN), which include 200 regions, comes in second.
- The third phase is the region based on R-CNN, which categorise all of the regions.
- These phases use a shared fully-convolutional network layer for feature extraction and classification in addition to region proposals.
- The initial training stage for images on a CNN for image categorization technique is a crucial step. Additionally, the regions suggested by calibratethe complete of this layer using RPN.
- Samples are given values by the initialise image classifier in the beginning phase. It will be noted that positive samples have IOU and that negative samples have IOU> threshold when these values exceed the IOU threshold.
- After processing the feature map of the complete image, it analyses a sliding tiny n * n spatial window. The sliding window, centre, ratio, and scale are all combined in the anchor. for example, k=9 anchors at each sliding position, 3 scales, 3 ratios, and. Initialising RPN training in FRCNN makes use of the shared convolutional layers.
- Therefore, it adjusts the layers that are special to RPNs. It will constantly tweak the distinctive Fast R-CNN layers. Then, if necessary to carry out the training and provide regional proposals.

The Faster R-CNN's overall design is shown in Fig. 4, which also shows that the network functions to detect objects. The Faster RCNN primarily collects the feature maps from CNN and sends to the RPN. The region proposal network RPN accepts inputs with different image sizes, and the outputs are a collection of rectangular object proposals. Next to CNN's last convolution layer, RPN is established. The final shared convolutional layer in CNN creates a region proposal network by sliding a tiny network over the output of the convolutional feature map. The input for this neural network is a $n \times n$ Spatial Window of the input convolutional feature map. Several simultaneous region proposals are projected at the location of each sliding window. The final CNN layer (sliding window) is transmitted by RPN to a smaller dimension of the feature map. The ROI pooling layer receives the RPN's recommendation, and the ROI pooling layer creates fixed-size feature maps from various input sizes. The parameters of the layer determine the output static dimension of the ROI pooling. Lastly, this feature is sent into the bcl and brl layers, which are also completely connected layers. As a regressor, a sophisticated bounding box is used, and the classifier assigns a classification to the lesions.

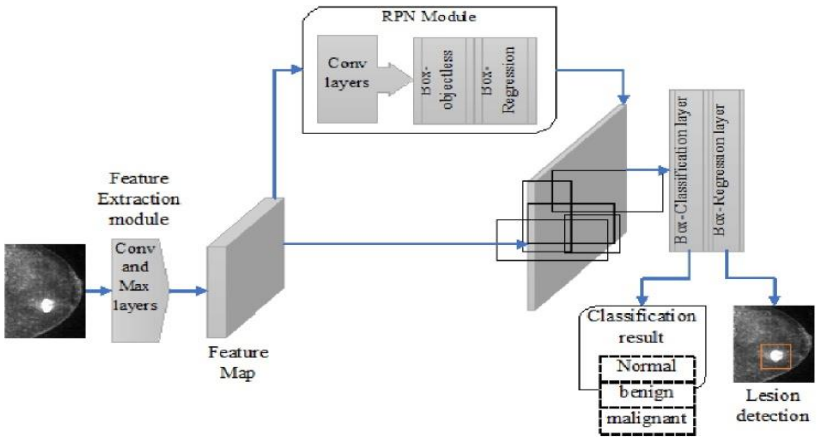

Fig.4. Working process of FRCNN method

FRCNN has the drawback that, in contrast to RPN, all the anchors in the minibatch are obtained from an individual image. Unfortunately, the recall using the validation dataset was low with a minimum score for true positives due to a network overfitting issue. In this research, the overfitting problem is solved through RMPA. The main hyperparameters such as Intersection Over Union (IOU), weight, batch size and epochs are modified to enhance the model's functionality were the initialization of weights and the optimizer.

RMPA:A recent MA called MPA mimics the phenomena of marine species searching for food. A predator is looking for prey, but the prey is looking for nourishment. The search process is divided into three phases based on the velocity relation between the predator and the prey. the term "aristocracy" refers to the predator with the strongest capacity for foraging. The ultimate goal of MPA, like similar swarm intelligence optimisation algorithms, is to find the best solution (aristocracy), in accordance with the planned position updating techniques. The specific usage is as follows:

Facet 1-High velocity:The predator updates the prey position by observing the prey's movement when its velocity ꝑ exceeds that of the predator $\left(it < \frac{\max it}{3}\right)$ while it is in a waiting state. This procedure takes place throughout the first third of iterations and is part of MPA's exploratory phase.

$$mꝑ_i = V_w \otimes (aristocracy_i - V_w \otimes ꝑ_i) \ \forall\ i = 1, \dots, n \quad (4)$$

Where $ꝑ_i = ꝑ_i + 0.5 \cdot rand \otimes mꝑ_i$

where aristocracy denotes the position of the aristocracy, ꝑdenotes the position of the prey, $n$denotes the size of the population, $V_w$denotes a vector based on wiener process, and $rand$denotes a random number in [0,1].

Facet 2-Entity velocity$\left(\frac{max\ it}{3} < it < \frac{2\max it}{3}\right)$**:**The prey adopts the Wiener process when its velocity is equal to that of the predator, whereas the aristocracy adopts the Lévy flight (LF) strategy. The procedure takes place in the MPA's exploration and exploitation phases in the middle of iterations. Utilising (5), the other half of the populace oversees exploration. The exploitative use of (6) is the responsibility of the other half.

$$mꝑ_i = V_{LF} \otimes (aristocracy_i - V_{LF} \otimes ꝑ_i) \quad (5)$$

Where $ꝑ_i = ꝑ_i + 0.5 \cdot rand \otimes mꝑ_i$.

$$mꝑ_i = V_w \otimes (V_w \otimes aristocracy_i - ꝑ_i) \quad (6)$$

Where $ꝑ_i = ꝑ_i + 0.5 \cdot AV \otimes mꝑ_i$ and

$$AV = \left(1 - \frac{it}{\max it}\right)^{2\left(\frac{it}{\max it}\right)}$$

where AV is an adaptive variable used to regulate a predator's step volume. Current iteration is represented by the variable it, while maximal iteration is represented by the variable maxit.

Facet 3-Low velocity: The predator's velocity is less than the prey $\left(it > \frac{2\,max\ it}{3}\right)$'s velocity in the final third of repetitions. The method's exploiting step is significantly extended.

$$mꝑ_i = V_{LF} \otimes (V_{LF} \otimes aristocracy_i - ꝑ_i) \quad (7)$$

Where $ꝑ_i = ꝑ_i + aristocracy_i \cdot AV \otimes mꝑ_i$

The effects of Fish Reckoning Devices (FRDs) are taken into consideration by MPA alongside to the previous three phases. Equation (8) is used to mimic the prey jumping with a specific probability from one setting to another. It can successfully stop the algorithm from getting stuck at the local optimum.

$$ꝑ_i = \begin{cases} ꝑ_i + AV[x_{min} + rand \otimes (x_{max} - x_{min}) \otimes VB] & if av \le FRD \\ ꝑ_i + [FRD \otimes (1 - rand) + rand](ꝑ_{r_1} - ꝑ_{r_2}) & else \end{cases} \quad (8)$$

Where FRDs=0.2,x_{min} and x_{max}denote the lower and upper boundaries,$ꝑ_{r_1}$ and $ꝑ_{r_2}$represent two random indexes of the prey. If the random integer in the range [0,1] is less than FRDs, the binary vector VB is composed of matrices that have both zero and one as entries. This is accomplished by creating a random vector av in the range [0,1] and updating

the array to zero if it is less than 0.2 and one if it is greater.

It is evident from a review of the classic MPA's efficiency that not all search space alternatives are sufficiently explored. Additionally, it has a poor convergence rate due to the splits the optimisation processes into three distinct parts. Thus, the hyperparameters of the pretrained FRCNN architecture are optimised utilising the original MPA that has been modified using the Opposition Based Learning (OBL) technique (RMPA). In order to enhance the search operation, the MPA's variety was increased during the initialization phase using the OBL technique as follows:

$$OB_s = \ell b_m + u b_m - \mathfrak{Y}_n \quad \forall m, n \in 1,2, \dots, N \ (9)$$

where $OB_s$is a vector produced by applying OBL, ℓb_m, and $u b_m$are lower and upper bounds of the mth component of $\mathfrak{Y}$, correspondingly. The following subsection provides a description of the suggested RMPA's phases.

Initialization steps in RMPA: Initialising the RMPA's parameters, population size N, FRDs, $rand$, and dimensions D, is the first step in the process. The MPA starts by saving outputs and initialising the first search agent $\mathfrak{Y}_0$. Then the starting population's OB_s is calculated by Equation (9) using the OBL technique.

Optimization processes: According to MPA, the optimisation process is split into three stages. The suggested technique updated the global best solution by determining and contrasting the fitness of $\mathfrak{Y}_n$ and OB_s after finishing these stages, which uses the OBL strategy to determine the fitness function for each solution in $\mathfrak{Y}$ and $\overline{\mathfrak{Y}}$.

Last steps in RMPA: Eq. (8) is used to calculate the FRDs after the optimisation process has been completed, memory has been saved, and Aristocracy has been updated. The prepared FRCNN architecture-based OFRCNN model is introduced in this part. To obtain the greatest efficiency out of the pretrained CNN model, the hyperparameters are optimised using the RMPA technique. A new test set is used to confirm the model once it has been trained. The fully trained model is subsequently validated using the test set. The pretrained FRCNN architecture's hyperparameters are optimised using the RMPA, which was fully trained using the hyperparameter values found in the second phase to assist the architecture correctly diagnose the test set in the third phase.

Experimental results and discussion

The suggested model is primarily divided into two phases: mass localization and then mass categorization. Some assessments are utilised to assess the precision of lesions detection, and others are employed to assess the efficacy of mass categorization. The model's accuracy in localising tumours in breast mammograms was assessed using the Intersection Over Union (IOU) measure as follows:

$$IOU = \frac{AO}{AU} \quad (10)$$

where AU stands for area of union and AO for area of overlap. If the IOU is larger than or equal to 0.5, the mass is considered properly identified; differently, the detection is disregarded. Each localised mass is put over a particular classifier to determine its kind of malignancy, and compared to the provided ground truth to yield one of four choices. The first is a benign mass that is properly recognised as benign (True Negative), followed by a benign mass that is mistakenly categorized as malignant (False Positive), a malignant mass that is categorized as malignant (TP), and finally a malignant mass that is properly categorized as benign (FN).The confusion matrix utilised to assess classification accuracy, is composed up mostly of these four variables. The comparative tools are the YOLO-V4 [13] and DLA-EABA [14] methods. Additionally, the subsequent calculations were made using the True Negative (TN) and True Positive (TP) measurements:

$$Precision = \frac{TP}{TP + FP} \quad (11)$$

$$Recall = \frac{TP}{TP + FN} \quad (12)$$

$$Overall\ accuracy = \frac{TP + TN}{TP + FN + TN + FP} \quad (13)$$

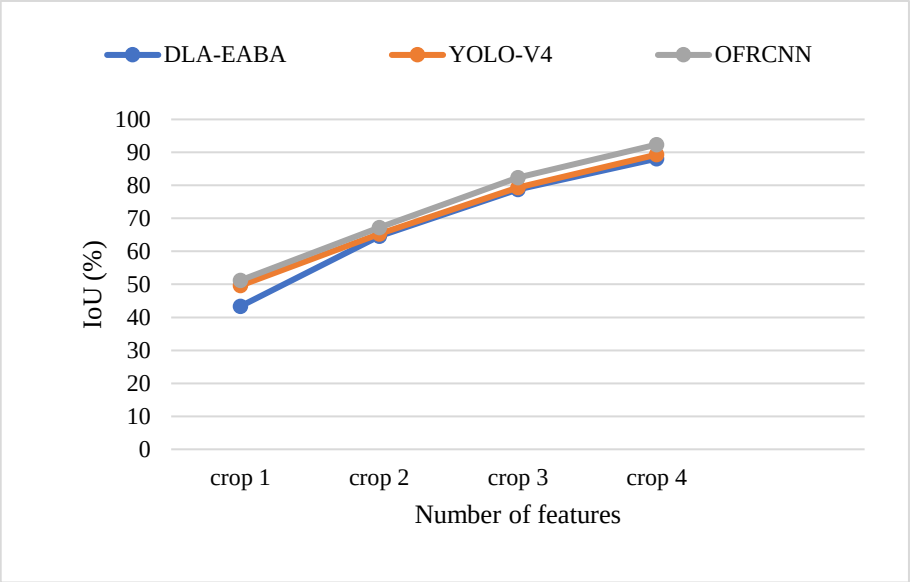

Fig.5. Precision performance comparison

Precision comparison results between suggested YOLO-V4, DLA-EABA and OFRCNN classifiers are shown in Fig.5. According to the graph, the suggested technique has a high IoU rate when With respect to current techniques. It is an efficient method of detecting attacks with a high IoU rate of 92.36%. When comparing the IoU of existing approaches, YOLO-V4 and DLA-EABA provide good precision rates of 88.09% and 89.32 %, respectively, which is lesser than the OFRCNN. Furthermore, the IoU of the RMPA method was used to pick the optimum hyperparameter values of FRCNN, resulting in a higher IoU rate

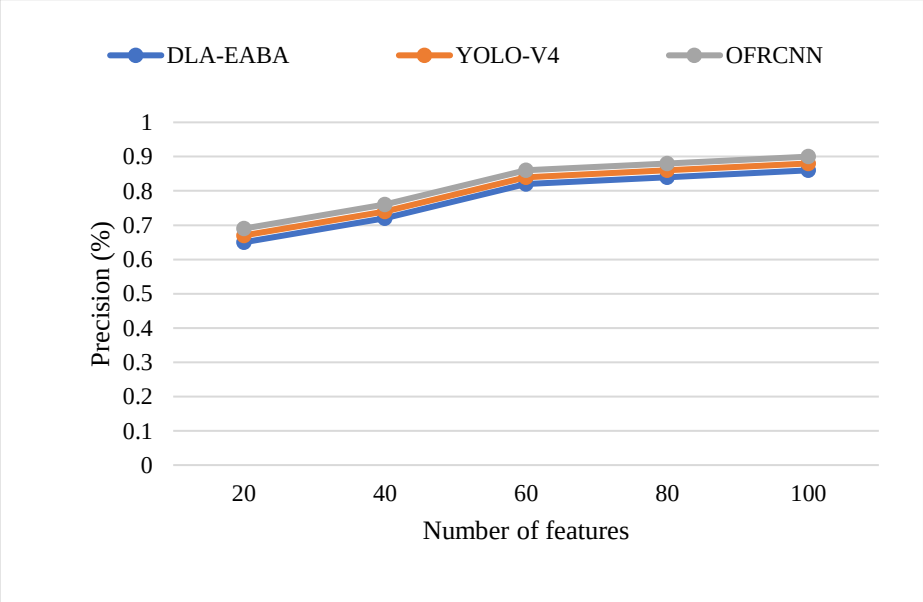

Fig.6. Precision performance comparison

The precision comparison results between suggested YOLO-V4, DLA-EABA and OFRCNN classifiers are shown in Fig.6. According to the graph, the suggested technique has a high precision rate when With respect to current techniques. It is an efficient method of detecting attacks with a high precision rate of 0.90%. When comparing the precision of existing approaches, YOLO-V4 and DLA-EABA provide good precision rates of 0.88% and0.86%respectively, which is lesser than the OFRCNN. The obvious difference between the fitness values at the beginning of the optimization process is because the RMPA uses the OBL method and thus improves the learning efficiency of OFRCNN.

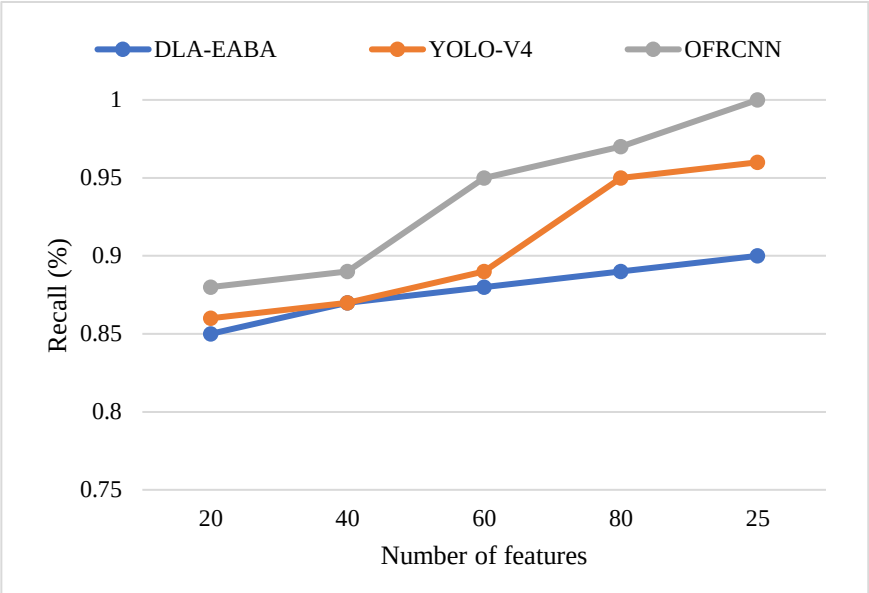

Fig.7. Recall performance comparison

The recall comparison results for suggested YOLO-V4, DLA-EABA and OFRCNNclassifiers are shown in Fig.7. The proposed approach offers an extremely high recall rate of 1%. According to the results, the suggested OFRCNNhas a high recall rate value, showing a good detection recognition accuracy. When comparing the recall rates of the existing approaches, YOLO-V4 and DLA-EABA provide recall rates of 0.96%, and0.9%, respectively, demonstrating that the suggested scheme can provide good disease recognition outcomes than the previous techniques.

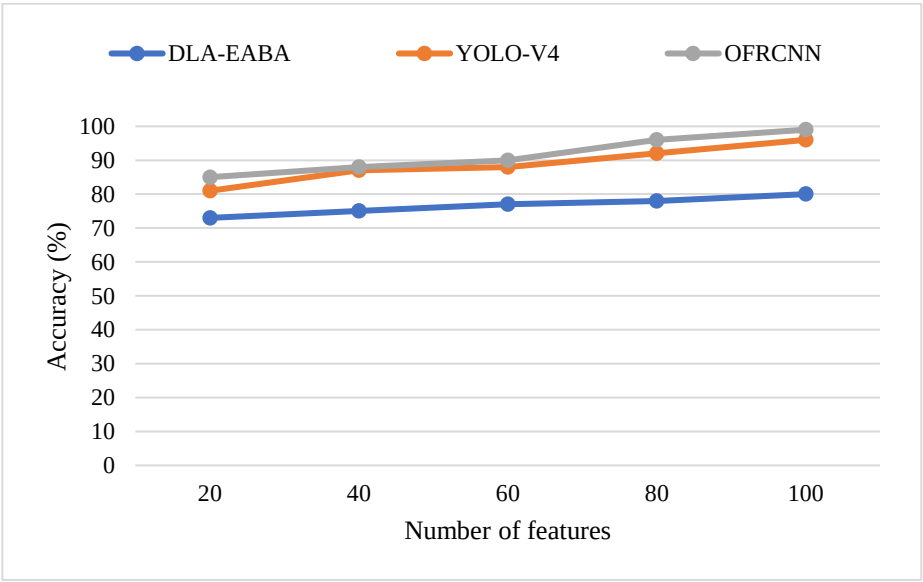

Fig.8. Accuracy performance comparison

The graph in Fig.8 above illustrates the accuracy comparison for attack detection. Methods such as YOLO-V4, DLA-EABA and OFRCNNclassifiers are used. OFRCNNis an excellent method for obtaining accurate predictions, with a high accuracy rate of 99%. When comparing the accuracy of previous techniques such as YOLO-V4 and DLA-EABA, the rates are as follows: 96%, and 80%, respectively. The local optima problem is eliminated while providing improved accuracy owing to the comparatively noise-resistant nature of OFRCNN learning algorithms. In addition, RMPA has a faster convergence capability than other techniques while preventing premature convergence, which raises the rate of BC identification.

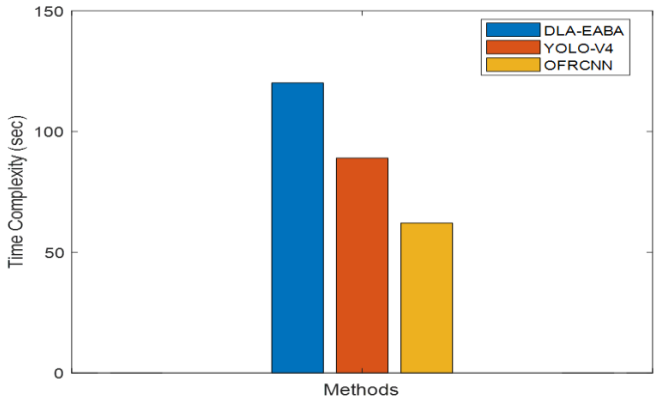

Fig.9. Execution time performance comparison

The graph in Fig.9 above illustrates the execution time comparison for attack detection. Methods such as YOLO-V4, DLA-EABA and OFRCNNclassifiers are used. OFRCNNis an excellent method for obtaining accurate predictions, with a lowexecution time rate of 62.116s. When comparing the execution time of previous techniques such as YOLO-V4 and DLA-EABA, the rates are as follows: 89.012s and120.14respectively. Since local optima and premature convergence are both eliminated by OFRCNN learning methods, BC detection rate is increased while execution time is kept to a minimum. By producing the bounding boxes that indicate tumours and their pathological kinds in less than 10 seconds, the suggested two identificationtechnique is a concurrentidentification and categorization technique that examinefor current masses in the screened PET / mammograms.

Conclusion and Future work

The suggested an OFRCNN-based CAD system to locate any potential cancerous breast tissue and, if present, accurately identify it as benign or malignant. This model suggested two detection methods, FPDP and CPDP, which might verify cases identified twice without requiring the time of radiologists. In order to prevent any reliance that can hinder the diagnosis process, the two pathways are applied in tandem. The first route oversees taking the complete PET after scaling it down to examinefor any masses.The second path is in charge of carrying out the same identification method by slicing the entire mammography into thin, overlapped slices, each of which is handled as a new case in which the model should look for tumours. This method finds lesions in the entire PET's cropped slices, and retrieved portions are combined to produce the full bounding box of any cancer that may already be present. The tiny tumours overlooked by the first identification path are successfully located by the second path in the suggested architecture. The suggested model increases the precision of detection of the lately presented CADs by reaching 99% for identification and acts as a concurrentsensor to identify and categorise existent masses in as little as a few seconds. In future, the network model structure and SSD (single shot detector) method for the tumour detection network enhanced, by applying model pruning, backbone structure optimisation, and reparameters.

References

1. Khokhar, A. (2012). Breast cancer in India: where do we stand and where do we go?. *Asian Pacific Journal of Cancer Prevention*, *13*(10), 4861-4866.
2. Nagrani, R. T., Budukh, A., Koyande, S., Panse, N. S., Mhatre, S. S., & Badwe, R. (2014). Rural urban differences in breast cancer in India. *Indian Journal of Cancer*, *51*(3), 277.
3. Gupta, S. (2016). Breast cancer: Indian experience, data, and evidence. *South Asian journal of cancer*, *5*(03), 085-086.
4. Sathwara, J., Bobdey, S., & Ganesh, B. (2016). Breast cancer survival studies in India: a review. *Int J Res Med Sci [Internet]*, *4*(8), 3102-8.
5. Juwle, A., & Saranath, D. (2012). BRCA1/BRCA2 gene mutations/SNPs and BRCA1 haplotypes in early-onset breast cancer patients of Indian ethnicity. *Medical oncology*, *29*(5), 3272-3281.
6. Mathur, P., Sathishkumar, K., Chaturvedi, M., Das, P., Sudarshan, K. L., Santhappan, S., ... & ICMR-NCDIR-NCRP Investigator Group. (2020). Cancer statistics, 2020: report from national cancer registry programme, India. *JCO Global oncology*, *6*, 1063-1075.
7. Vaka, A. R., Soni, B., & Reddy, S. (2020). Breast cancer detection by leveraging Machine Learning. *ICT Express*, *6*(4), 320-324.
8. Ahmed, I., & Devulapally, P. (2022). Nuclear Medicine PET Scan Cardiovascular Assessment,

Protocols, And Interpretation. In *StatPearls [Internet]*. StatPearls Publishing.
9. Zebari, D. A., Ibrahim, D. A., Zeebaree, D. Q., Haron, H., Salih, M. S., Damaševičius, R., & Mohammed, M. A. (2021). Systematic review of computing approaches for breast cancer detection based computer aided diagnosis using mammogram images. *Applied Artificial Intelligence*, *35*(15), 2157-2203.
10. Yassin, N. I., Omran, S., El Houby, E. M., & Allam, H. (2018). Machine learning techniques for breast cancer computer aided diagnosis using different image modalities: A systematic review. *Computer methods and programs in biomedicine*, *156*, 25-45.
11. Priyanka, K. S. (2021). A review paper on breast cancer detection using deep learning. In *IOP conference series: materials science and engineering* (Vol. 1022, No. 1, p. 012071). IOP Publishing.
12. Wu, N., Phang, J., Park, J., Shen, Y., Huang, Z., Zorin, M., ... & Geras, K. J. (2019). Deep neural networks improve radiologists' performance in breast cancer screening. *IEEE transactions on medical imaging*, *39*(4), 1184-1194.
13. Hamed, G., Marey, M., Amin, S. E., & Tolba, M. F. (2021). Automated Breast Cancer Detection and Classification in Full Field Digital Mammograms Using Two Full and Cropped Detection Paths Approach. *IEEE Access*, *9*, 116898-116913.
14. Zheng, J., Lin, D., Gao, Z., Wang, S., He, M., & Fan, J. (2020). Deep learning assisted efficient AdaBoost algorithm for breast cancer detection and early diagnosis. *IEEE Access*, *8*, 96946-96954.
15. Wang, Z., Li, M., Wang, H., Jiang, H., Yao, Y., Zhang, H., & Xin, J. (2019). Breast cancer detection using extreme learning machine based on feature fusion with CNN deep features. *IEEE Access*, *7*, 105146-105158.
16. Nagalakshmi, T. (2022). Breast Cancer Semantic Segmentation for Accurate Breast Cancer Detection with an Ensemble Deep Neural Network. *Neural Processing Letters*, 1-14.
17. Bhausaheb, D. P., & Kashyap, K. L. (2022). Detection and classification of breast cancer availing deep canid optimization based deep CNN. *Multimedia Tools and Applications*, 1-19.
18. Oyetade, I. S., Ayeni, J. O., Ogunde, A. O., Oguntunde, B. O., & Olowookere, T. A. (2022). Hybridized deep convolutional neural network and fuzzy support vector machines for breast cancer detection. *SN Computer Science*, *3*(1), 1-14.
19. Chattopadhyay, S., Dey, A., Singh, P. K., Oliva, D., Cuevas, E., & Sarkar, R. (2022). MTRRE-Net: A deep learning model for detection of breast cancer from histopathological images. *Computers in Biology and Medicine*, *150*, 106155.
20. Beeravolu, A. R., Azam, S., Jonkman, M., Shanmugam, B., Kannoorpatti, K., & Anwar, A. (2021). Preprocessing of breast cancer images to create datasets for deep-cnn. *IEEE Access*, *9*, 33438-33463.
21. Erkut, U., Bostancıoğlu, F., Erten, M., Özbayoğlu, A. M., & Solak, E. (2019, November). HSV color histogram based image retrieval with background elimination. In *20191st international Informatics and Software Engineering Conference (UBMYK)* (pp. 1-5). IEEE.
22. Sim, W. Y., Park, N. H., & Kwon, T. J. (2021). Unusual sonographic appearance of breast cancer metastasis to the pectoralis muscle. *Journal of Clinical Ultrasound*, *49*(8), 881-884.
23. Liu, J., Malekzadeh, M., Mirian, N., Song, T. A., Liu, C., & Dutta, J. (2021). Artificial intelligence-based image enhancement in pet imaging: Noise reduction and resolution enhancement. *PET clinics*, *16*(4), 553-576.
24. Li, Z., Zheng, J., & Zhu, Z. (2014, July). Content adaptive guided image filtering. In *2014 IEEE International Conference on Multimedia and Expo (ICME)* (pp. 1-6). IEEE.
25. Jyotiyana, M., & Kesswani, N. (2021). Introduction to Deep Learning in Health Informatics. *Biomedical Data Mining for Information Retrieval: Methodologies, Techniques and Applications*, 237-261.
26. Jain, D. K. (2019). An evaluation of deep learning based object detection strategies for threat object detection in baggage security imagery. *pattern recognition letters*, *120*, 112-119.
27. Wang, W., & Shen, J. (2017). Deep cropping via attention box prediction and aesthetics assessment. In *Proceedings of the IEEE international conference on computer vision* (pp. 2186-2194).
28. Naveen, B., & Nandeesh, M. (2022). FRCNN Algorithm Strategy with Image Cropping for Dental Radiographs. In *Proceedings of the International Conference on Cognitive and Intelligent Computing* (pp. 535-542). Springer, Singapore.